The Application of Input Shaping to a System with Varying Parameters

David P. Magee, Graduate Student
Dr. Wayne J. Book, Professor
George W. Woodruff School of Mechanical Engineering
Georgia Institute of Technology
Atlanta, Georgia

Abstract

The original input shaping technique developed by Singer and Seering is summarized and a different definition for residual vibration is proposed. The new definition gives better insight into the ability of input shaping method to reduce vibration. The extension of input shaping to a system with varying parameters, e.g. natural frequency, is discussed and the effect of these variations is shown to induce vibration. A modified command shaping technique is developed to eliminate this unwanted motion.

Introduction

The industrial and environmental applications for robots with a relatively large workspace has increased significantly in the last few years. To accommodate the demands, the manipulator is usually designed with long, lightweight links which are inherently flexible. This flexibility allows the links to store potential energy which is returned to the system in the form of kinetic energy. Therefore, the end-point vibration, which affects the uncertainty in end-point position, is directly related to the flexibility of the links.

Many different methods, both passive and active, have been investigated to eliminate unwanted oscillation to improve end-point positioning capabilities. The most crude passive approach to eliminate vibration is to simply wait for vibrations to stop after a desired motion. NASA originally used this method on their Space Shuttle Remote Manipulator System but found it to be very costly in task completion time requirements. Other passive approaches include applying a thin layer of visco-elastic material to absorb energy, using piezo-resistive films to resist beam motion and various vibration absorption techniques [1,2,3].

The majority of the present day techniques involve active control structures to minimize end-point vibration. Different states of the system are measured and conventional feedback schemes are used to control the vibration. Hastings and Book [4] extended active control methods by including strain feedback in the control structure. They showed that strain feedback can reduce residual vibration during settling time. However, they conclude that the vibrations are inevitable with a feedback control scheme because feedback control signals contain high frequency components, which excite the system resonances.

Another method to reduce vibration is the use of inertial devices. Montgomery, Ghosh and Kenny [5] propose torque-wheel actuators to reduce overshoot in the Space Shuttle Remote

Manipulator. Their results indicate that the wheel can produce a vibration of significant amplitude to diminish the original unwanted vibration. Lee and Book [6] are studying the effects of inertial forces to suppress vibration by mounting a small robot at the tip of a large, flexible robot. Using deflection rate control, the small robot generates damping forces to accommodate the inertial forces generated at the tip.

The technique that is discussed in this paper involves the modification of a command signal so that the system resonances are not excited. The idea of command altering is not a new one. O.J.M. Smith [7] suggested the use of posicast control which takes a step of a given amplitude and separates it into two smaller steps, one of which is separated in time. This method was shown to reduce the settling time of the system. Meckl and Seering [8] examined the construction of the input from a series expansion of ramped sinusoid functions with coefficients chosen to minimize a spectral magnitude. The results were reduction in residual vibration even for variations in resonant frequencies.

Singer and Seering [9,10,11] presented a method of generating shaped command inputs that utilizes system characteristics. Each sample of the desired input is transformed into a new set of impulses that do not excite the system resonances. This procedure, in effect, filters out frequency components near the system's resonance to avoid vibration during motion. However, their experiments were limited to systems with constant parameters. The ability of the method to accommodate slight deviations in system parameters is handled by the derivation of robustness constraints. To fully appreciate the method, a more detailed discussion is warranted.

The Input Shaping Technique

The original input shaping method developed by Singer and Seering is best explained by considering the motion of a flexible system as the linear combination of flexible and rigid body motion. The rigid body motion can be modeling using conventional methods, e.g. Newton, Lagrange, etc., and consider representing the flexible motion as a simple, second-order system. The vibratory response of a linear, time-invariant, underdamped second-order system to an impulse can be written as

$$x(t) = \frac{A \omega_n e^{-\zeta \omega_n (t - t_0)}}{\sqrt{1 - \zeta^2}} \sin\left(\omega_n \sqrt{1 - \zeta^2} \, (t - t_0)\right) \tag{1}$$

where A is the amplitude of the impulse, ω_n is the natural frequency of the system, ζ is the damping ratio of the system, t is the time and t_0 is the time when the impulse occurs. Since the input shaping technique generates a set of new impulses, the response of the second-order system to two impulses can be expressed as

$$x(t) = B_1 \sin(\alpha t + \phi_1) + B_2 \sin(\alpha t + \phi_2) \tag{2}$$

where

$$B_k = \frac{A_k \omega_n}{\sqrt{1 - \zeta^2}} e^{-\zeta \omega_n (t - t_{0k})} \tag{3}$$

$$\alpha = \omega_n \sqrt{1 - \zeta^2} \tag{4}$$

$$\phi_k = -\omega_n t_{0k} \sqrt{1 - \zeta^2}. \tag{5}$$

The response of the system to the two impulse input can be simplified to yield

$$x(t) = B_{amp} \sin(\alpha t + \psi) \tag{6}$$

$$B_{amp} = \sqrt{[B_1 \cos(\phi_1) + B_2 \cos(\phi_2)]^2 + [B_1 \sin(\phi_1) + B_2 \sin(\phi_2)]^2} \tag{7}$$

$$\psi = \tan^{-1} \left(\frac{B_1 \sin(\phi_1) + B_2 \sin(\phi_2)}{B_1 \cos(\phi_1) + B_2 \cos(\phi_2)} \right). \tag{8}$$

Since the system is linear and time-invariant, the results from Equations (7) and (8) can be generalized to the N impulse case. The resulting amplitude and phase for the response are

$$B_{amp} = \sqrt{\left[\sum_{k=1}^{N} B_k \cos(\phi_k) \right]^2 + \left[\sum_{k=1}^{N} B_k \sin(\phi_k) \right]^2} \tag{9}$$

$$\psi = \tan^{-1} \left(\frac{\sum_{k=1}^{N} B_k \sin(\phi_k)}{\sum_{k=1}^{N} B_k \cos(\phi_k)} \right). \tag{10}$$

Since the purpose of the input shaping method is to eliminate vibration, the amplitude of vibration given in Equation (9) must equal zero after the last input impulse occurs in time. This only happens if both the squared terms are independently zero since the sine and cosine functions are linearly independent. The resulting equations are

$$B_1 \cos(\phi_1) + B_2 \cos(\phi_2) + \dots + B_N \cos(\phi_N) = 0 \tag{11}$$

$$B_1 \sin(\phi_1) + B_2 \sin(\phi_2) + \dots + B_N \sin(\phi_N) = 0. \tag{12}$$

Simplifying Equations (11) and (12) yields the zeroth-order constraint equations given by

$$\sum_{k=1}^{N} A_k e^{-\zeta \omega_n (t_N - t_{0k})} \cos(\omega_n \sqrt{1 - \zeta^2} \, t_{0k}) = 0 \tag{13}$$

$$\sum_{k=1}^{N} A_k e^{-\zeta \omega_n (t_N - t_{0k})} \sin(\omega_n \sqrt{1 - \zeta^2} \, t_{0k}) = 0. \tag{14}$$

For the constraint equations to produce the correct impulse sequence to eliminate vibration, the natural frequency and damping ratio of the system must be exact. Since these system characteristics are never precisely known, a robustness constraint is added. The robustness constraints are found by taking the partial derivatives of Equations (13) and (14) with respect to ω_n or ζ and setting the result equal to zero. Higher derivative constraints are obtained by differentiating the equations to the desired order. The mth-derivative robustness constraints are

$$\sum_{k=1}^{N} A_k (t_{0k})^m e^{-\zeta \omega_n (t_N - t_{0k})} \cos(\omega_n \sqrt{1 - \zeta^2} \, t_{0k}) = 0 \tag{15}$$

$$\sum_{k=1}^{N} A_k (t_{0k})^m e^{-\zeta \omega_n (t_N - t_{0k})} \sin(\omega_n \sqrt{1 - \zeta^2} \, t_{0k}) = 0. \tag{16}$$

The length of the impulse sequence is now determined by the number of unknowns in a given set of constraint equations. For any given set, there will always be two more unknowns than equations. To alleviate this dilemma, the starting time of the first impulse is chosen to be time zero and the amplitudes of the impulses are normalized so that they sum to unity. This particular normalization ensures that the overall amplitude of the new impulse sequence is the same as the amplitude of the desired input command.

Example of Two Impulse Case

For the two impulse case, the zeroth-order constraint equations are utilized, which are

$$B_1 \cos(\phi_1) + B_2 \cos(\phi_2) = 0 \tag{17}$$

$$B_1 \sin(\phi_1) + B_2 \sin(\phi_2) = 0. \tag{18}$$

Since any equation involving sines and cosines is transcendental, there are an infinite number of possible solutions to Equations (17) and (18). Therefore, only the solution that yields the shortest time duration and a positive amplitude for all the impulses is chosen. The solution is

$$A_1 = \frac{1}{1+M} \tag{19} \qquad\qquad t_{01} = 0 \tag{20}$$

$$A_2 = \frac{M}{1+M} \tag{21} \qquad\qquad t_{02} = \frac{\pi}{\omega_n \sqrt{1-\zeta^2}} \tag{22}$$

where

$$M = e^{-\frac{\zeta \pi}{\sqrt{1-\zeta^2}}}. \tag{23}$$

Equation (22) states that the second impulse occurs in time at one-half the damped period of the system. This seems reasonable to apply an impulse to oppose the vibration of the system. The ability of the input shaping method to eliminate vibration can be demonstrated graphically. Consider the input given in Figure 1 whose characteristics are given in Equations (19) thru (22).
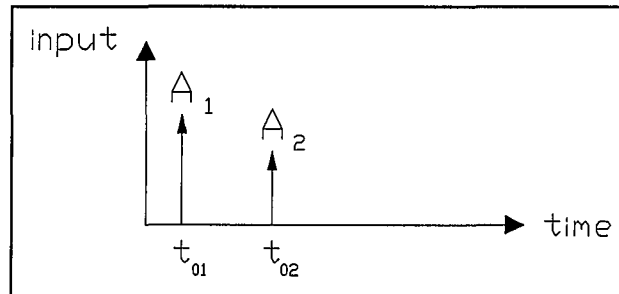

Figure 1. Two Impulse Input

The second-order system response to each of the impulses in Figure 1 is shown in Figure 2.
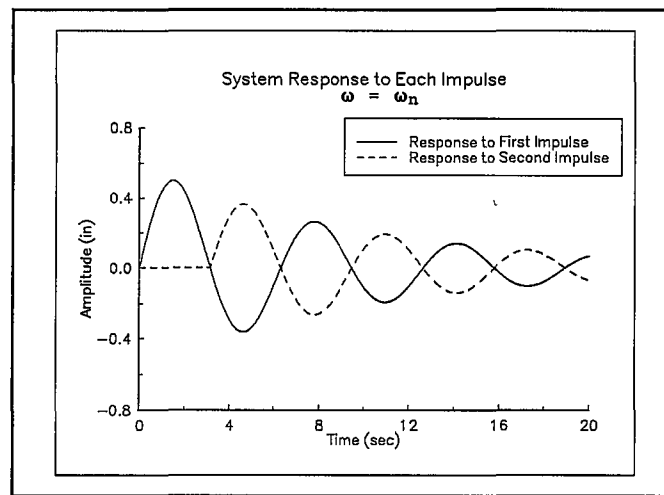

Figure 2. System Response to Each Impulse

Since the system is linear and time-invariant, a linear combination of two inputs results in a response that is a linear combination of the two responses. Therefore, the net system response to the two impulse input is shown in Figure 3. Since the natural frequency and damping ratio
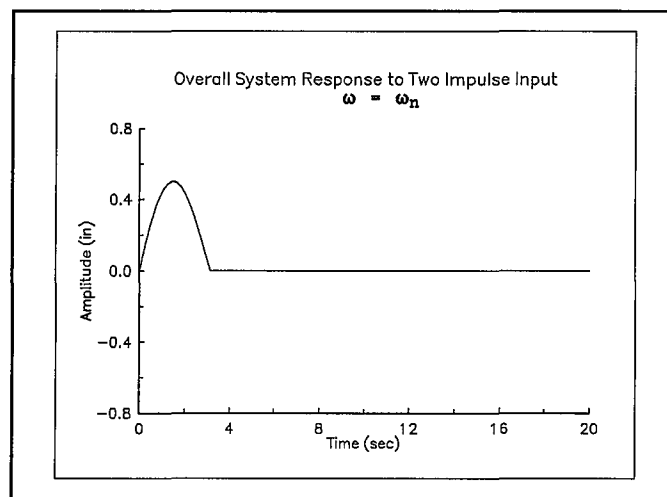

Figure 3. Overall System Response to Two Impulse Input

are exact, there is no vibration of the system after the second impulse occurs. The flexible motion has been eliminated and all that remains is rigid body motion.

Robustness of Constraint Equations

The previous example demonstrated the ability of the input shaping method to eliminate vibration when the natural frequency and damping ratio of the system were known exactly. For most physical systems, the exact parameters are seldom known. Thus, there is some residual vibration after the last impulse has occurred. To determine the amount of residual vibration, a new vibration error expression must be defined. The error, denoted *err*, is expressed as the ratio of the actual multiple impulse response magnitude to the actual impulse response magnitude of the second-order system. The error expression is defined only for time after the multiple impulse input has occurred to ensure that the system has received identical amplitude inputs, i.e. the inputs sum to the same value. Mathematically, the vibration error is written as

$$err = \frac{|x_{ka}(t)|}{|x_a(t)|} \quad , \quad for \quad t \geq t_{0k} \tag{24}$$

where k is the number of impulses. The residual vibration is just the vibration error expressed as a percentage.

The deviation of the actual system parameters from the design parameters can now be quantified using Equation (24). By studying the deviations in natural frequency and damping ratio from the design parameters, their effects on vibration error can be better understood. To demonstrate this point, again considered the two impulse input case. The vibration error from Equation (24) is found to be

$$\frac{|x_{2a}(t)|}{|x_a(t)|} = \left| \frac{1}{M+1} \sqrt{1 + 2M^{\left(1-\frac{\omega_a}{\omega_n}\right)} \cos\left(\frac{\omega_a}{\omega_n}\pi\right) + M^{2\left(1-\frac{\omega_a}{\omega_n}\right)}} \right| \tag{25}$$

where ω_a is the actual natural frequency of the system and ω_n is the design natural frequency of the system. Figure 4 shows the vibration error as a function of normalized frequency, ω_a/ω_n and Figure 5 displays Singer's original vibration error. The two principal differences between the definitions are evident when comparing the figures:

1. The magnitudes achieved by the residual vibration

2. The behavior of the residual vibration with respect to damping ratio

From Singer's definition, the magnitude of the residual vibration never exceeds 100%. This phenomenon implies that the input shaping method will never increase the residual vibration of the system no matter the variation in natural frequency. Clearly, this is cannot be the case. One can envision applying the second impulse at a time equal to the damped period of the system. Figure 6 reveals a second-order system response to a single impulse input compared with a two impulse input when the actual natural frequency is twice the design natural frequency. The residual vibration after the second impulse is actually worse than if the system had only been given the single impulse. Therefore, the input shaping method can have a detrimental effect
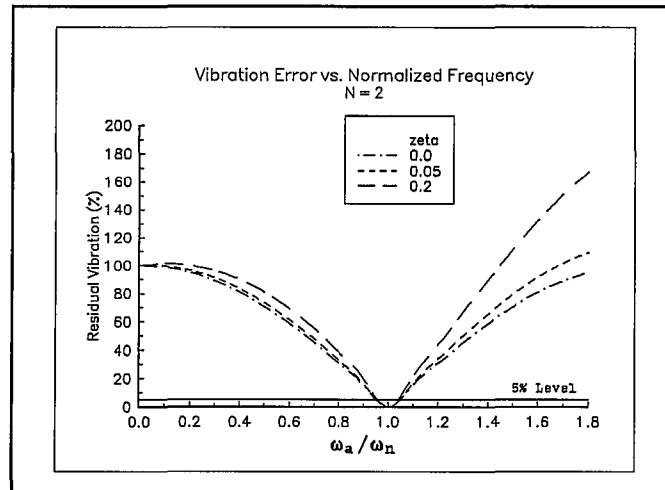
Figure 4. Vibration Error vs. Normalized
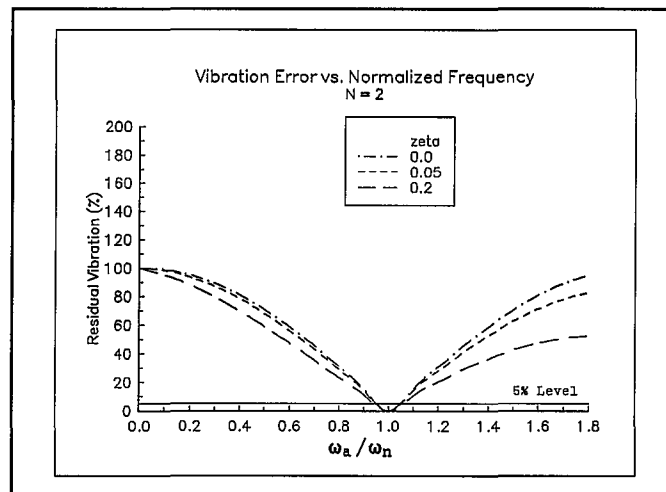Frequency - Two Impulse Input

Figure 5. Vibration Error vs. Normalized
Frequency - Singer's Definition

when large errors in natural frequency occur.

The second difference deals with the relationship between the damping ratio and the residual vibration. The new definition shows that the residual vibration increases for an increase in damping ratio. This fact may seem incorrect since the overshoot of a second-order system decreases with an increase in damping ratio. However, manipulation of Equation (1) for different values of damping ratio (at a constant value of natural frequency) reveals that the amplitude of the impulse response increases for larger values of damping ratio.
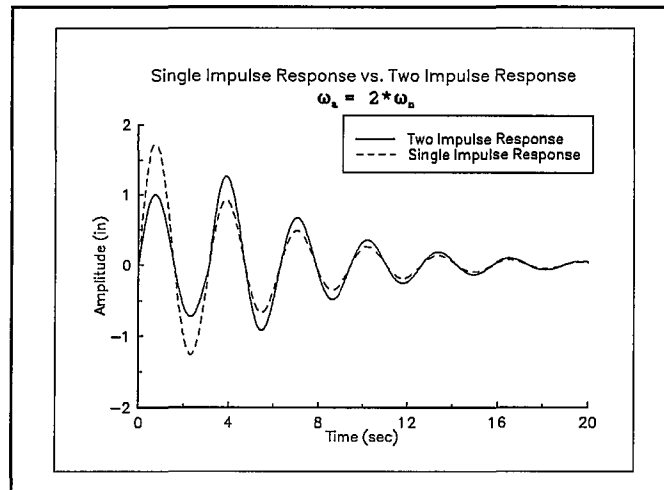
Figure 6. Single Impulse Response vs. Two Impulse
Response

One final note regarding the vibration error is the robustness of the two impulse input. Singer defines an acceptable vibration error level of less than 5% residual vibration for the second-order system. After reviewing Figure 4, the two impulse input is robust only for a frequency variation of less than 5%. To improve the robustness with respect to natural frequency, more impulses must be used. By solving the higher order derivative constraints mentioned previously, the amplitudes and starting times of more impulses can be found. After solving set of equations, the vibration error can be calculated. The vibration error graphs for the case of three and four impulses are shown in Figures 7 and 8, respectively. Notice that the robustness for variations in natural frequency increases for more impulses but there is a larger penalty in residual vibration if the parameters are outside the acceptable level.

The robustness with respect to damping ratio can also be pursued by evaluating the vibration error equation for variations in damping ratio. Singer states that the higher order derivative constraints also satisfy variations in damping ratio so the derivation will not be addressed here. The only point to make is that large variations in damping ratio do not have a significant effect on the residual vibration. This fact is comforting since the damping ratio of a complex system can be difficult to measure.

Position Dependent Parameters

The robustness of the constraint equations demonstrated the ability of the input shaping method to reduce vibrations even with deviations from the design parameters. However, the method does not consider the issue of changing system parameters. For many flexible, robot systems, the natural frequency and damping ratio are functions of position, e.g. joint angles. Therefore, a modified command shaping technique is developed to accommodate this deficiency.

To develop this new method, the implementation of the input shaping technique to a discrete-time system is presented. Figure 9 shows a simple block diagram of the input shaping
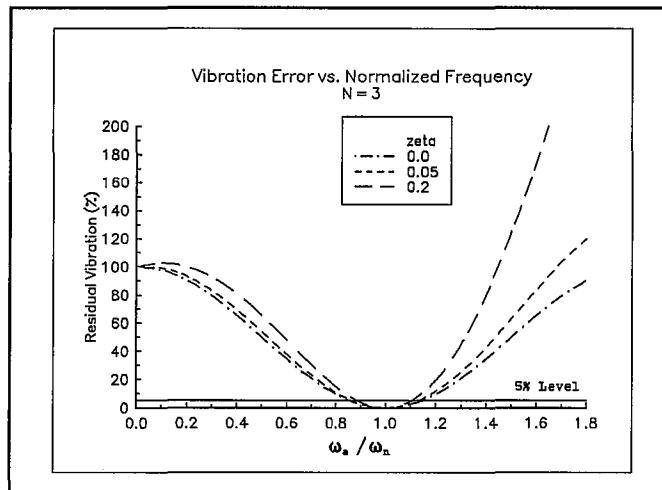
Figure 7. Vibration Error vs. Normalized
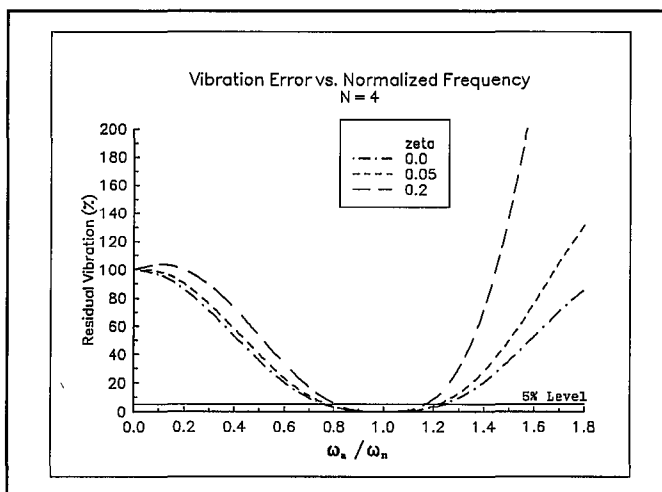Frequency - Three Impulse Input

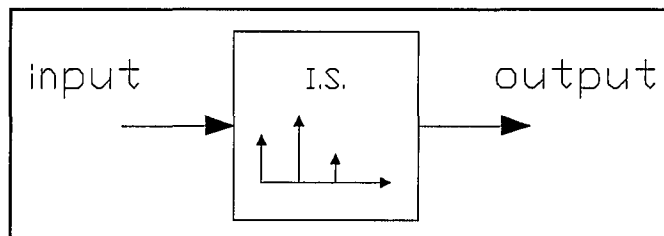Figure 8. Vibration Error vs. Normalized
Frequency - Four Impulse Input

Figure 9. Input Shaping Block Diagram

method. For each sample of the desired input, N output impulses are generated. The output impulses are equally spaced in time with a continuous-time period, denoted *delT*,

$$delT = \frac{\pi}{\omega_n \sqrt{1 - \zeta^2}} \qquad (26)$$

which is a function of both the natural frequency, ω_n, and damping ratio, ζ. To utilize this time period information in a discrete-time system, the continuous-time data must be represented in discrete-time. From discrete-time signal processing, a continuous-time signal, x(t), is represented mathematically as a sequence of numbers, x[n], where n is strictly an integer. To transform the continuous-time period *delT* into a discrete time period *deln*, the sampling rate of the discrete-time system, f_s, is used. The equation to perform this transformation is

$$deln = int(delT * f_s) \qquad (27)$$

where the *int* function truncates its argument to an integer.

For the input shaping method, the discrete-time period, *deln*, never changes because the system parameters are assumed constant. But when the input shaping method is applied to a system that has time varying parameters, the continuous-time period, *delT*, becomes time varying as well. A significant change in *delT* will result in a change in the discrete-time period, *deln*, which produces an undesirable vibration in the system. The amount of change in the continuous period that causes this change in the discrete period is a function of sampling rate since *deln* is strictly an integer.

For example, consider the input shaping method shown in Figure 9 that produces four new impulses for each sample of the desired input. Assuming that the discrete-time period evaluates to an integer value of four, the method would produce a steady-state impulse output shown in Figure 10. Each output impulse is designated {a,b} where a indicates the discrete-time location of the input sample responsible for the four output impulses and b indexes the four resulting output impulses. Now assume that the system configuration has changed enough to alter the value of the discrete-time period. Figure 11 shows the steady-state impulse output for a change in the discrete-time period, *deln*, from four to five. After examining Figure 11, it is obvious that the change in *deln* has caused gaps in the output for discrete values of n. At $n=4$, for example, only three impulses are contributing to the overall output. To make matters worse, this problem is repeated five more times at a discrete-time period near the system's natural period. This phenomenon induces a vibration into the system that is caused solely by the application of the input shaping method to a system with time varying parameters.

This induced vibration is also present when the value of *deln* decreases. Consider a change in *deln* from five to four. The resulting steady-state impulse output is shown in Figure 12. For this situation, a surplus of output impulses is generated at a discrete-time period near the system's natural period. These extra impulses also cause a vibration that is produced by the input shaping method.

To eliminate the induced vibration, a modified command shaping method is proposed to make the impulse output more uniform when a change in *deln* is encountered. To compensate for a change in the discrete-time period, extra impulses are added for an increase in *deln* and impulses are removed for a decrease in *deln*. The choice of which impulses are affected is based

on the number of output impulses from the shaping algorithm and the old and new values of the discrete-time period.

Modified Command Shaping

The modified command shaping method can be explained by designating the discrete-time value when the discrete period increases as $n=0$. For the next N-1 samples of the input, i.e. $0 \leq n \leq N$-2, the modified command shaping technique shapes each sample using both the old and new values of *deln* to create a smooth steady-state impulse output. Using the new value of *deln*, the input sample is shaped to create N output impulses that are added to the overall output at their respective discrete-time values. Using the old value of *deln*, the same input sample is also shaped to create N output impulses. However, only the last N-$(n+1)$ output impulses are added to the steady-state output at their respective discrete-time values. For discrete-time values of $n \geq N$-1, each sample of the input is shaped normally using the new value of *deln* to generate the N output impulses.

The modified command shaping method also works for a decrease in the discrete-time period, *deln*. For this situation, the input sample is shaped only once using the new value of *deln* to produce the four output impulses. Instead of adding all four of the output impulses, only the first $(n+1)$ output impulses are added to the steady-state output at their respective discrete-time values. By manipulating the overall output in this way, the extra impulses that are added for the case when *deln* increases are the same impulses that are removed when *deln* decreases.

One final case to consider is when the value of *deln* changes more than once within one discrete-time period. For this situation, a new modified technique must be devised. For instance, if the discrete-time period length changes from one value to another and back again, the best method to smooth the steady-state output may be to ignore the change in discrete period if it is relatively short.

To understand the modified command shaping procedure, consider the example given in Figure 11. The value of *deln* increases from four to five for this input shaping scheme that produces four output impulses. Since $N=4$ for this case, the next three (i.e. N-1) input samples will be shaped twice. At discrete-time $n=0$, the input sample is shaped using the new value of *deln* (i.e. 5) to create four (i.e. N) output impulses that are added to the overall output. At the same discrete-time value, the input sample is shaped using the old value of *deln* (i.e. 4) to create four (i.e. N) output impulses. However, only the last three (i.e. N-$(n+1)$) impulses are added to the overall output at their respective discrete-time values. For the next discrete-time value, i.e. $n=1$, the input sample is shaped using the new value of *deln* to create the usual four output impulses that are added to the overall output. When the input sample is shaped using the old value of *deln*, only the last two (i.e. N-$(n+1)$) output impulses are added to the general output. This process of shaping the input samples twice is repeated until the discrete-time value, n, is greater that N-2. After $n > N$-2, the shaping continues normally using only the new value of *deln* to produce the output impulses. The steady-state impulse output for an increase in discrete-time period using the modified command shaping is shown in Figure 13. The impulses due to the modified method are darkened to show emphasis only.

The application of the modified command shaping method to a decrease in discrete-time period is much simpler. Considering the example in Figure 12, the steady-state impulse output from the modified method is given in Figure 14. The impulses that are created but not added

-2,1	-1,1	0,1	1,1	2,1	3,1	4,1	5,1	6,1	7,1	8,1	9,1	10,1	11,1	12,1	13,1	14,1	15,1	16,1
-6,2	-5,2	-4,2	-3,2	-2,2	-1,2	0,2	1,2	2,2	3,2	4,2	5,2	6,2	7,2	8,2	9,2	10,2	11,2	12,2
-10,3	-9,3	-8,3	-7,3	-6,3	-5,3	-4,3	-3,3	-2,3	-1,3	0,3	1,3	2,3	3,3	4,3	5,3	6,3	7,3	8,3
-14,4	-13,4	-12,4	-11,4	-10,4	-9,4	-8,4	-7,4	-6,4	-5,4	-4,4	-3,4	-2,4	-1,4	0,4	1,4	2,4	3,4	4,4

n	-2	-1	0	1	2	3	4	5	6	7	8	9	10	11	12	13	14	15	16
deln	4	4	4	4	4	4	4	4	4	4	4	4	4	4	4	4	4	4	4

Figure 10. Steady-State Output for Constant Discrete-Time Period Using Input Shaping

-2,1	-1,1	0,1	1,1	2,1	3,1		5,1	6,1	7,1			10,1	11,1				15,1	16,1
-6,2	-5,2	-4,2	-3,2	-2,2	-1,2	4,1	0,2	1,2	2,2	8,1	9,1	5,2	6,2	12,1	13,1	14,1	10,2	11,2
-10,3	-9,3	-8,3	-7,3	-6,3	-5,3	-4,3	-3,3	-2,3	-1,3	3,2	4,2	0,3	1,3	7,2	8,2	9,2	5,3	6,3
-14,4	-13,4	-12,4	-11,4	-10,4	-9,4	-8,4	-7,4	-6,4	-5,4	-4,4	-3,4	-2,4	-1,4	2,3	3,3	4,3	0,4	1,4

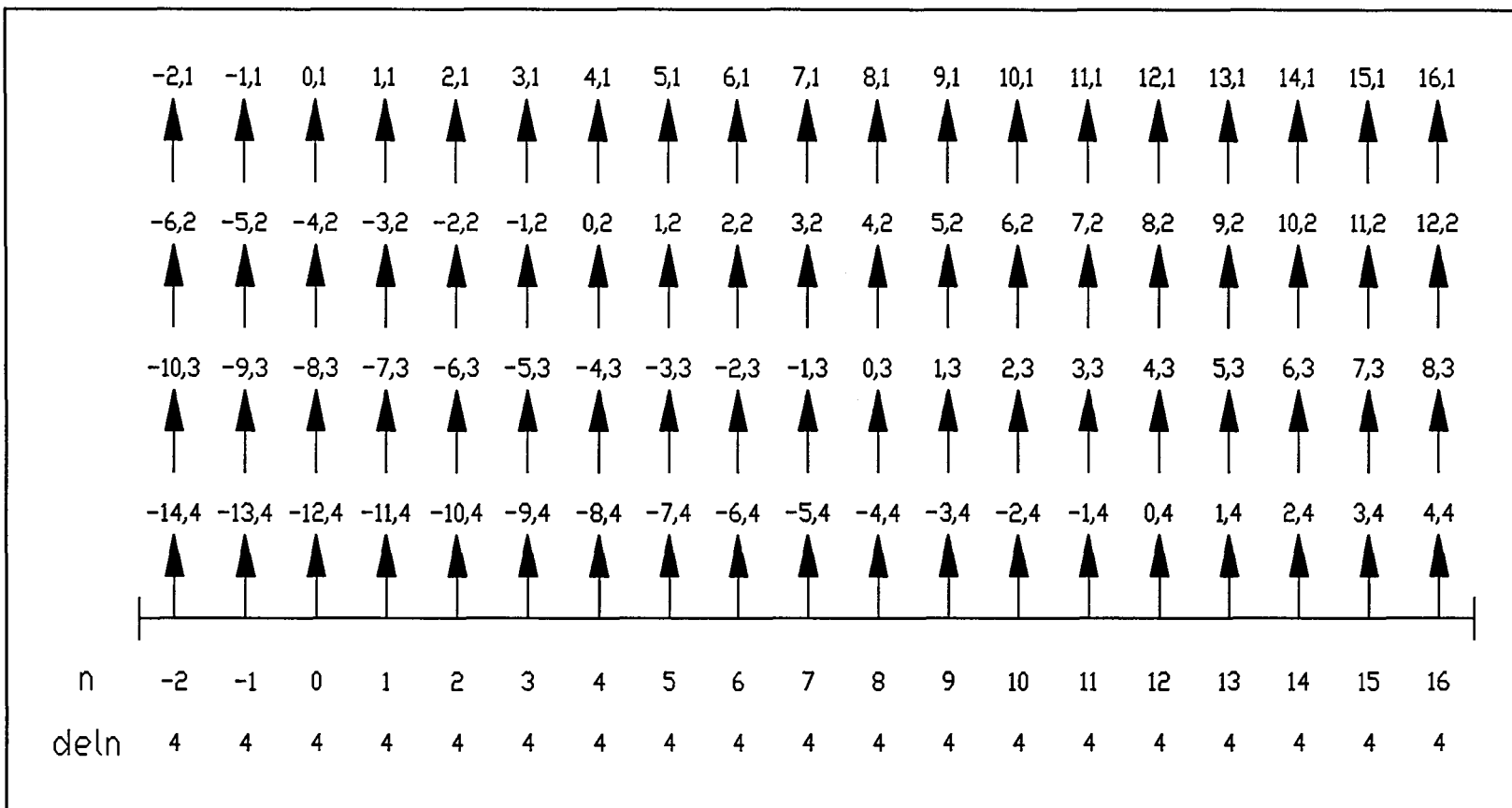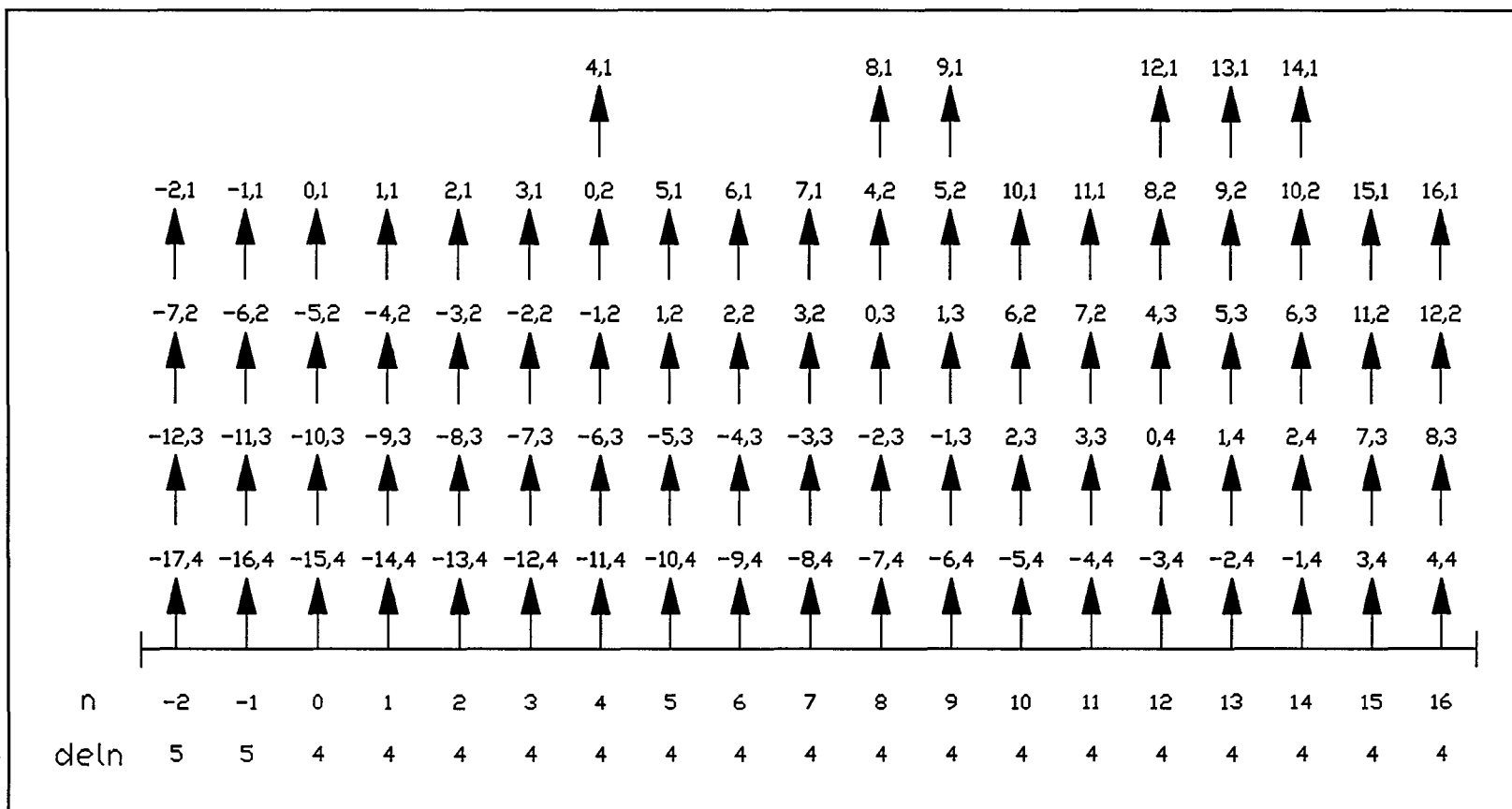| n	-2	-1	0	1	2	3	4	5	6	7	8	9	10	11	12	13	14	15	16
deln	4	4	5	5	5	5	5	5	5	5	5	5	5	5	5	5	5	5	5

Figure 12. Steady-State Output for a Decrease in Discrete-Time Period Using Input Shaping

Figure 13. Steady-State Output for an Increase in Discrete-Time Period Using Modified Command Shaping

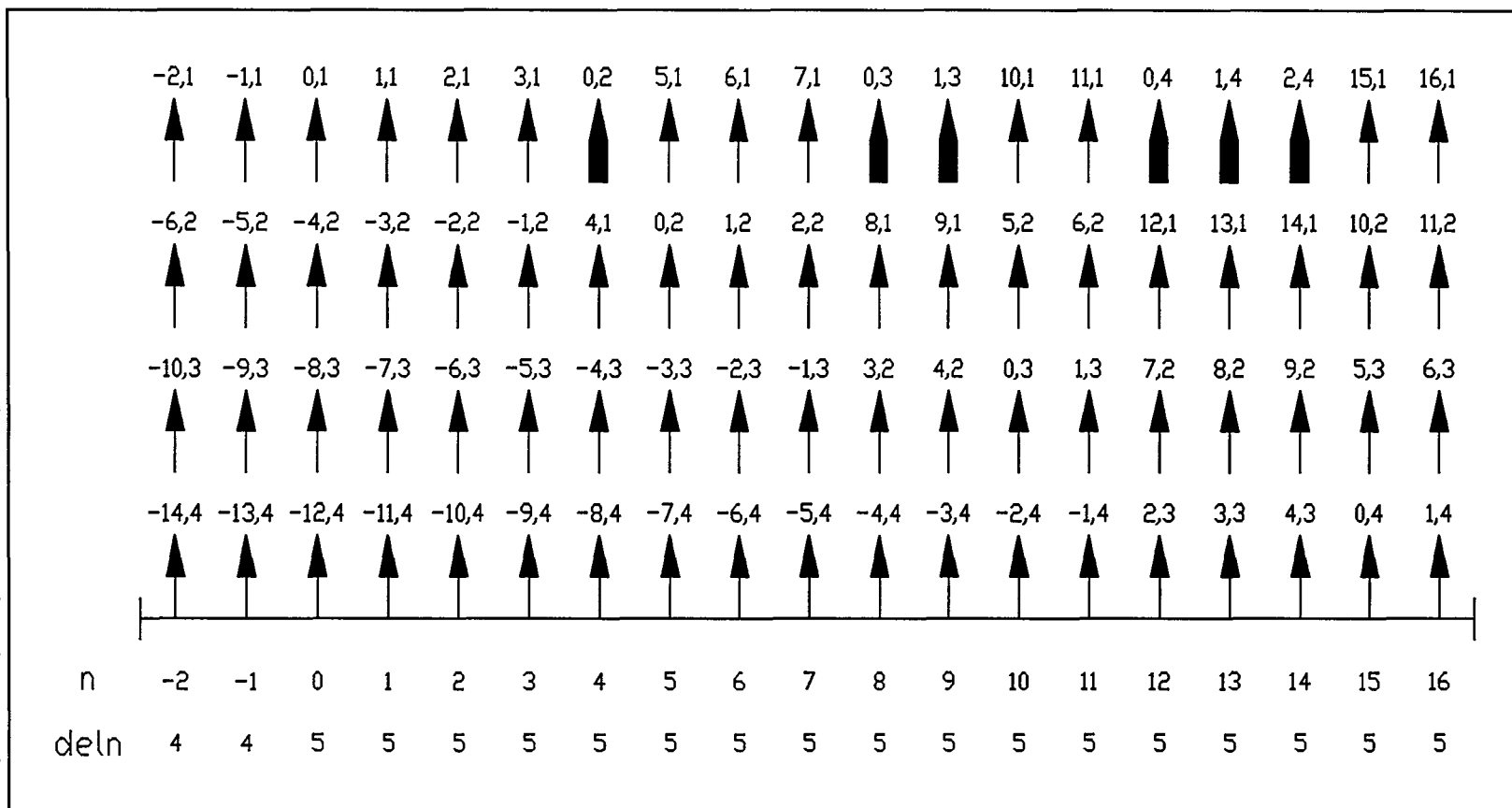| n	-2	-1	0	1	2	3	4	5	6	7	8	9	10	11	12	13	14	15	16
(row 1)	-2,1	-1,1	0,1	1,1	2,1	3,1	0,2	5,1	6,1	7,1	0,3	1,3	10,1	11,1	0,4	1,4	2,4	15,1	16,1
(row 2)	-6,2	-5,2	-4,2	-3,2	-2,2	-1,2	4,1	0,2	1,2	2,2	8,1	9,1	5,2	6,2	12,1	13,1	14,1	10,2	11,2
(row 3)	-10,3	-9,3	-8,3	-7,3	-6,3	-5,3	-4,3	-3,3	-2,3	-1,3	3,2	4,2	0,3	1,3	7,2	8,2	9,2	5,3	6,3
(row 4)	-14,4	-13,4	-12,4	-11,4	-10,4	-9,4	-8,4	-7,4	-6,4	-5,4	-4,4	-3,4	-2,4	-1,4	2,3	3,3	4,3	0,4	1,4
deln	4	4	5	5	5	5	5	5	5	5	5	5	5	5	5	5	5	5	5

Figure 14. Steady-State Output for a Decrease in Discrete-Time Period Using Modified Command Shaping
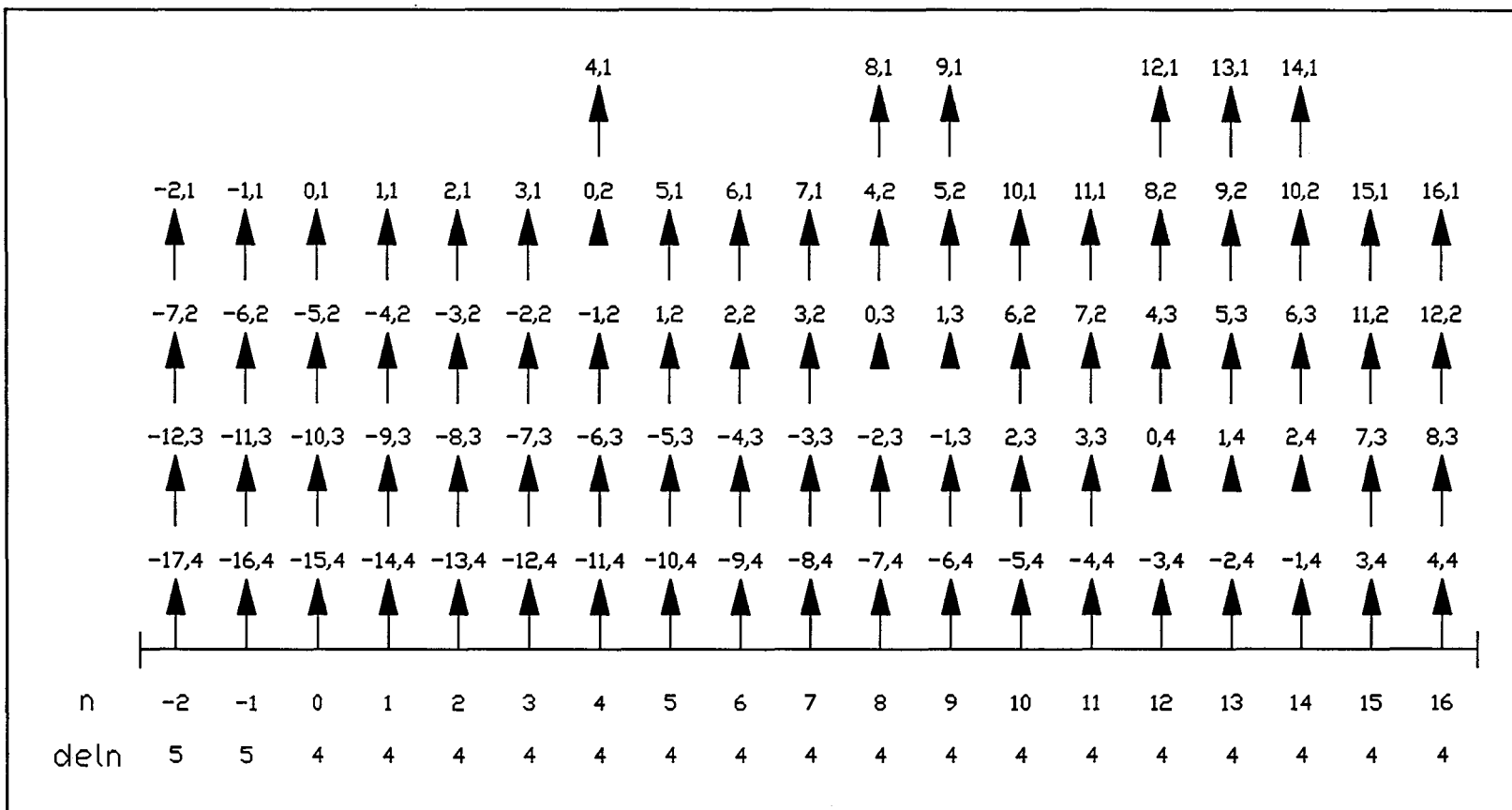
are drawn in the figure without tails to distinguish them from the normal impulses. Notice that the extra impulses that are added for the increase in discrete-time period are the same impulses, i.e. the same indices, that are eliminated for a decrease in discrete-time period. Although the amplitudes of the impulses are not exactly the same (since they originated from different samples of the desired input), this method provides a unique means for maintaining continuity of the steady-state output impulses.

Experimental Verification of Induced Vibration

To verify that the input shaping method does induce vibration for variations in discrete-time period, the method was applied to an existing adaptive P.D. control strategy developed by Yuan [12] that controls a two DOF flexible manipulator (RALF) located at Georgia Tech. The block diagram of the comprehensive control scheme is shown in Figure 15.
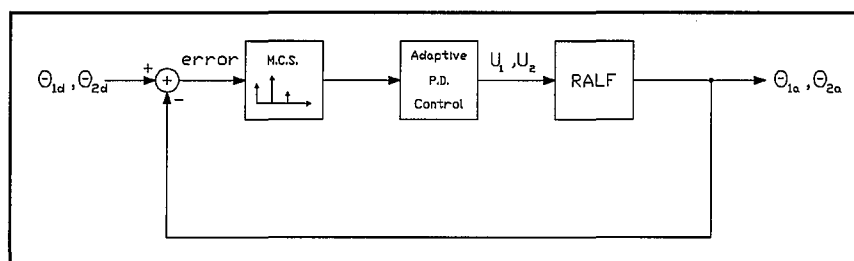

Figure 15. Block Diagram of Control System

The main control unit is a MicroVAX II containing A/D boards that can sample a single channel at 6000 Hz. However, the boards are limited to 300 Hz if multiple channels are accessed. After the computation time of the control routines is considered, the sampling frequency is reduced to 50 Hz. This sampling rate is acceptable since the first natural frequency of RALF that is to be controlled ranges from 3.7 to 5.5 Hz.

To demonstrate the elimination of the induced vibration, a desired trajectory in joint space is precomputed to ensure an equivalent basis for comparison. For this example, the desired path is a circle in cartesian space that is three feet in diameter with a period of nine seconds. An accelerometer is mounted at the tip of the robot to measure transverse vibration of the second link. The robot is commanded to follow the desired trajectory eight times which allows for reliable averaging of the data. A HP Signal Analyzer records the time response of the accelerometer and computes the frequency response of the data.

Figure 16 shows a comparison of the frequency response between the original P.D. control routine without command shaping and the original input shaping method of Singer's substituted for the modified command shaping method in Figure 15. Notice that the frequency response of the input shaping method is greater than for the P.D. routine alone. At the frequency range the input shaping method is designed to control (3.7-5.5 Hz), the response is 12 dB larger. This is due to a change in the discrete-time period which induces vibration at the system resonances. It is also worth pointing out that the second resonance of RALF occurs near 10 Hz and is evident in the frequency response.
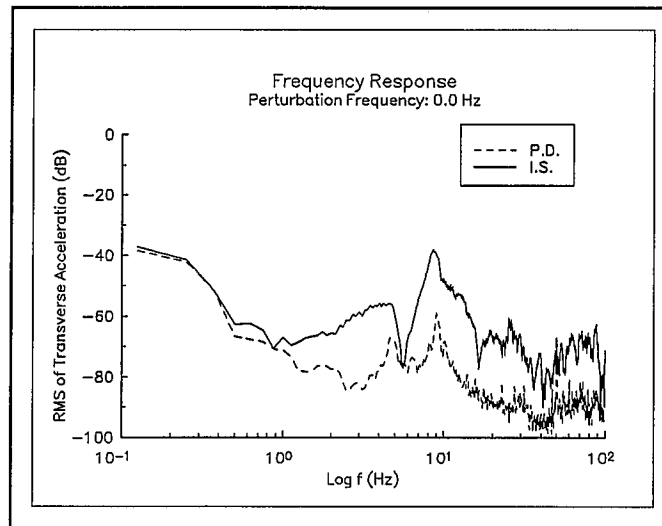
Figure 16. Frequency Response of RALF
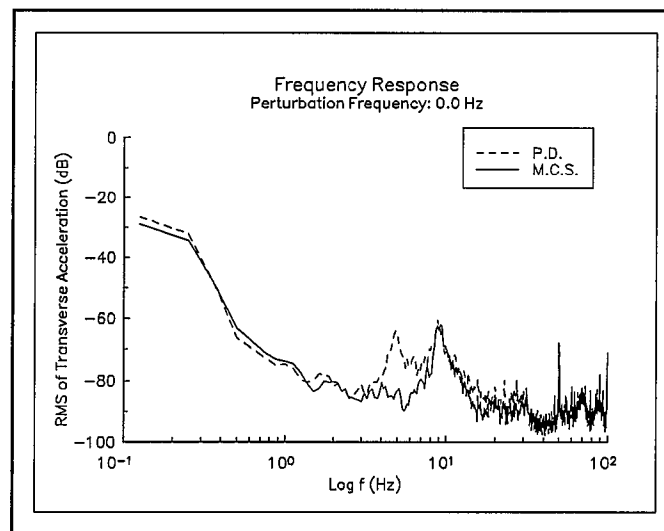P.D. vs. Input Shaping

Figure 17. Frequency Response of RALF
P.D. vs. Modified Command Shaping

Figure 17 compares the frequency response between the P.D. routine and the modified command shaping method. The modified command shaping has reduced the magnitude of the resonant vibration by 20 dB compared to the original P.D. routine. Therefore, this modified method reduced the vibration by nearly 32 dB over the input shaping method. Again, this increase in performance is due to the inability of the input shaping method to accommodate a change in the discrete-time period. A visualization method that clearly shows the induced vibration can be found in [13].

Conclusion

The original input shaping method developed by Singer and Seering was presented and robustness criterion described. A different vibration error expression was presented and shown to better represent the ability of the method to reduce residual vibration. The input shaping method was shown to induce vibration in systems with varying parameters and a modified command shaping technique was developed. The ability of the modified method to eliminate the induced vibration was shown using frequency response analysis of the transverse vibration of the tip of a flexible manipulator.

References

1. Alberts, T.E., Hastings, G.G., Book, W.J. and Dickerson, S.L., "Experiments in Optimal Control of a Flexible Arm with Passive Damping," *Fifth VPI&SU/AIAA Symposium on Dynamics and Control of Large Structures*, Blacksburg, VA, 1985.

2. Bailey, T. and Hubbard, J.E.,"Distributed Piezoelectric-Polymer Active Vibration Control of a Cantilever Beam," *Journal of Guidance and Control*, September-October, 1985, pp. 605-611.

3. Tewani, S.G., Walcott, B.L. and Rouch, K.E., "Active Optimal Vibration Control using Dynamic Absorber," *Proceedings of the 1991 International Conference on Robotics and Automation*, Sacramento, CA, pp.1182-1187.

4. Hastings, G.G. and Book, W.J., "Experiments in the Optimal Control of a Flexible Manipulator," *Proceedings of the 1988 American Control Conference*, Boston, MA, pp.728-729.

5. Montgomery, R.C., Ghosh, D. and Kenny, S., "Analytic and Simulation Studies on the Use of Torque-Wheel Actuators for the Control of Flexible Robotic Arms," to appear in the 1991 ASME Winter Annual Meeting, Atlanta, GA.

6. Lee, S.H. and Book, W.J., "Use of End-Effector Inertial Forces for Damping the Vibration of a Large Arm," *Proceedings of the 1989 American Control Conference*, Philadelphia, PA, pp.1377-1380.

7. Smith, O.J.M., "Feedback Control Systems," McGraw-Hill, 1958.

8. Meckl, P.H. and Seering, W.P., "Reducing Residual Vibration in Systems with Time-Varying Resonances," *Proceedings of the 1887 IEEE International Conference on Robotics and Automation*, Raleigh, NC, pp. 1690-1695.

9. Singer, N.C. and Seering, W.P., "Preshaping Command Inputs to Reduce System Vibration," AIM No. 1027, The Artificial Intelligence Laboratory, Massachusetts Institute of Technology, January, 1988.

10. Singer, N.C. and Seering, W.P., "Design and Comparison of Command Shaping Methods for Controlling Residual Vibration," *Proceedings of the 1989 IEEE International Conference on Robotics and Automation*, Scottsdale, AZ, pp.888-893.

11. Singer, N.C., *Residual Vibration Reduction in Computer Controlled Machines*, Ph.D. Thesis, Massachusetts Institute of Technology, February, 1989.

12. Yuan, B.S., *Adaptive Strategies for Controls of Flexible Arms*, Ph.D. Thesis, Georgia Institute of Technology, April, 1989.

13. Magee, D.P., *Dynamic Control Modification Techniques in Teleoperation of a Flexible Manipulator*, Masters Thesis, Georgia Institute of Technology, November, 1991.